WAVE EMISSIONS FROM PLANETARY MAGNETOSPHERES

Final Report for Grant NAGW-827

or the period

June 1, 1985 to May 31, 1989

Principal Investigator: Crockett L. Grabbe

Department of Physics

University of Iowa

Iowa City, IA 52242

FINAL REPORT FOR NASA GRANT NAGW-827

for research on

PLASMA WAVES AND INSTABILITIES IN PLANETARY MAGNETOSPHERES

Broadband Electrostic Noise in the Magnetotail

An important recent development in the Earth's magnetosphere has been the discovery of the boundary of the plasma sheet and its apparent role in the dynamics of the magnetotail. This boundary layer is where energetic ion beams reside, where electron currents often occur, and where the most intense waves in the magnetotail -- broadband electrostatic noise (BEN) -- is generated. It also may be the primary transport region in the magnetotail [Eastman, et al. 1984; Grabbe and Eastman, 1984].

Our initial research in this area provided the first evidence that broadband electrostatic waves was generated by ion beams in the plasma sheet boundary [Grabbe and Eastman, 1984]. The original paper attempted to explain the data through an ion beam model with only one instability, but later work under this grant showed 3 instabilities are present [Grabbe, 1984; 1985a; 1985b; 1986b] and are the generation mechanism for these waves. Our early research and results stimulated a significant amount of research by other scientists on the generation mechanism and its consequences [Ashour-Abdalla, et al., 1986; Akimoto and Omidi, 1986; Dusenberry; 1987; Shriver and Ashour-Abdalla, 1987; Nishikawa, et al., 1987].

We have investigated the detailed nature of these 3 instabilities through analytical and numerical studies of their frequency and growth rate as a function of angle of propagation. The first instability is the negative energy mode instability in which an ion acoustic mode is propagating on the ion beam in an opposite direction to the beam (commonly known as the ion acoustic instability) and generates the components at angles in a large cone centered about the magnetic field line. An analytical solution for the mode was first presented in Grabbe [1985b].

A second instability that contributes to the broadband electrostatic noise spectrum is the counterstreaming instability produced by the ion beams. This instability occurs at a large angle to the magnetic field but for a narrow angular range, and was identified by Akimoto and Omidi [1986] as the ion-ion 2-stream instability. The instabillity generally has much larger growth rates than the ion acoustic instability, and can generate much lower frequencies than the latter can. It generates the lowest frequencies of BEN. For typical plasma sheet boundary conditions the angle of this instability is around 75 degrees, close to observations to determine the polarization of the BEN spectrum at lower frequencies (100 Hz) a decade ago. [Gurnett and Frank, 1976; Grabbe, 1985a,b; 1986b; 1987a,b].

Analysis of the effect of the cold component of the electrons showed that they are responsible for producing the high frequency part of the spectrum. They cause a third instability to occur: the positive energy ion-electron two stream instability (commonly called the Buneman instability), which occurs for waves propagating in a narrow cone centered about the magnetic field line.

The most probable source of this population of electrons is diffusion in from the lobe into the plasma sheet boundary layer, so the instability should be concentrated close to the interfact between the boundary layer and the lobe. The presence of the Buneman instability component can explain why part of the spectrum gets very near the plasma frequency, higher than can be produced by the hot components alone. This fact along with the concentration of this component along the field explains why the components appears quite strongly and suddenly when the spacecraft enters the PSBL [Grabbe 1985a,b; 1986b; 1987a,b,c].

Our research on the generation of broadband electrostatic noise has provided a foundation for understanding certain processes occuring in the magnetotail. Comparison with wave propagation effects in the data supports the theory that 3 instabilities are present in the observed waves [Grabbe, 1987a]. Preliminary research implies it plays an important role in the transport which is occuring in the magnetotail [Grabbe and Eastman, 1984; Ashour-Abdallah and Okuda, 1986].

Resonance Cones in Space Plasmas

We have completed the inital analysis of a new theory for certain unidentified waveforms involving arches of decreasing frequency with time picked up in the Voyager II flyby of Uranus [Gurnett et al., 1986]. These modes have the characteristic that they rapidly drop down in frequency from their initial value of about 1.1 kHz to its final value of about 0.7 kHz in a matter of a few seconds.

The explanation we have proposed for these waveforms involves resonance cones that can occur for radiation in that mode from localized sources. These have been a major area of research in recent years [Mosier and Gurnett, 1969; Fisher and Gould, 1971; James, 1976; Ohnuma, 1978; Balmain, 1979; Grabbe, 1989]. What occurs is that under certain plasma conditions for a given wave frequency the electrostatic part of the wave becomes totally concentrated on the surfaces of two outgoing cones from the source, while the electronagnetic component is more isotropically distributed. These surfaces lie on cones ("resonance cones") along certain angles with respect to the magnetic field direction for a given frequency.

We have interpretated the waves observed at Uranus as resonance cone emissions from such a source band of frequencies, with the moving spacecraft changing the source-antenna angle and thus the source frequency received. The frequency of the received wave rapidly drops. Only for a short time is the spacecraft at appropriate resonance cone angles for receiving the observed band of frequencies emitted by the source.

In the homogeneous analysis it was found that the frequency detected on the spacecraft should drop almost linear in time. When the homogeneous theory is valid one can use the wave frequencies to identify the distance and angle of the source, and such predictions were made from the observed waveforms. This may provide valuable insights into how the waves are generated [Grabbe, 1988a; 1988b].

In general important effects will be introduced in the spectrum from the

effects of inhomogeneities in the plasma density and magnetic field, and from the thermal effects on the resonance cones. Analyses using more sophisticated models with simplifying assumptions on the inhomogeneous and thermal effects have been initiated. These appear be capable of explaining features observed on the waveforms such as multiple peaks and sudden variations in waveform slopes. Furthermore, an apparent modulation of one of the waveforms may result from an Alfven wave local to the spacecraft. [Grabbe, 1988b; Grabbe, 1989]

In addition to the natural occurence of resonance cone phenomena in wave generated in space environment, resonance cones can be an important part of active experiments for generating waves in space or the laboratory. It is well known that when small sources or antennas are used to generate or launch waves in a plasma, the waves tend to propagate in the form of resonance cones (in which the electrostatic components of the waves tend to be concentrated along certain group velocity directions.) Two aspects of this phenomenon have been explored: the application to the difficult problem of wave propagation in bounded inhomogeneous plasmas, and the general problem and application of waves excited by pulsed antennas in plasmas.

A model problem on the full-wave solution of waves excited by a small gap source in an inhomogeneous plasma with a lower-hybrid resonance layer present has been solved [Grabbe, 1985d]. The plasma model was a two-dimensional one bounded on both sides in one direction and free in the other, which is also the magnetic direction. Such a configuration supports guided waves, but the approach used was that involving resonance-cone forms of the solution. This approach is a mathematically equivalent but physically complementary point of view, and for the inhomogeneous problem is more tractable analytically [Grabbe, 1980]. The results show that the resonance-cone approach makes a much closer contact with the physics than the guided-wave approach for this case. Furthermore, the solution exhibits a significant mathematical elegance in that the rather complex individual resonance cone terms contributing to the total solution lend themselves to a physical diagrammatic interpretive scheme.

This model problem is of interest to wave propagation in plasma cavities in space environments, such as that of AKR trapped in density cavities in the auroral zone, where the inhomogeneous plasma contains resonance and cutoff layers for the AKR. It is also relevant to the problem of wave heating of laboratory plasmas for fusion research.

An investigation on the problem of the response of a magnetized plasma to a pulsed antenna has also been made [Grabbe, 1985e]. The initial analysis was made for a cold plasma because of the considerable difficulties involved in the warm plasma case. The result is that the plasma oscillates at three characteristic discrete frequencies: the upper hybrid frequency and the two frequencies that correspond to the two branches of the resonance cones for the given angle of observation with respect to the magnetic field.

In addition, the results of the calculation predict the amplitudes of these three responses as a function of the plasma density, magnetic field, pulse length, and observation angle with respect to the magnetic field. The interesting aspect of this result is that by measuring the relative response frequencies and their relative amplitudes created by a pulsed antenna in any magnetized plasma, one can determine the four parameters mentioned (plasma

density, magnetic field, pulse length, and observation angle). Thus this may provide a diagnostic for space plasmas if spectrum analyzers are available that can provide the needed data sufficiently fast.

Chorus-Associated Electrostatic Bursts

Reinleitner et al. [1982, 1983] recently published data showing the generation of electrostatic waves by electrons trapped in the wave packets of chorus waves. They propose the explanation that the phase velocity of the chorus wave packet changes with the local plasma conditions, resulting in acceleration of the trapped particles. This shifts the trapped particles in velocity space, so that they produce a "bump" (beam) superimposed on the untrapped or background electrons. A beam instability results that can drive electrostatic waves.

The analysis of Grabbe [1985a] used a finite temperature beam, and Maxwellians for the background electrons and ions, which fit the observed distribution functions much better than previous models. It was shown that although the proposed explanation of the origin of the electrostatic bursts appears to be supported and correct, the identification of the instability mechanisms involved was incorrect. It was found that the electron-ion two-stream instability is most likely the dominant mechanism.

Langmuir Turbulence in Space Plasmas

Langmuir turbulence occurs in several instances in space plasmas, such as in planetary bow shocks. A study was made of the case of the Jovian bow shock a few year ago, and it was shown that the Langmuir waves were generated by electrons bouncing off the shock, and evolves into a turbulence [Gurnett et al, 1981]. An advance in some aspects of the theory of Langmuir turbulence through the Zakharov equations has aided our understanding of some of these phenomena. [Zakharov, 1971]. An overview of plasmas in space where Langmuir turbulence occurs and its relation to the theory of Langmuir turbulence has been published under this grant [Grabbe and Sheerin, 1985].

Resource Book on Plasma Waves and Instabilities

One of the difficulties for the space plasma physics community has been that of having ready access to and awareness of material containing results of investigations of problems of wave propagation, radiation, instabilities, and turbulence that has been produced by the plasma fusion and laboratory plasma research community. While the general physics is often quite similar, the plasma parameters and the language may differ considerably. This often results in the creation of a barrier between the two groups of plasma scientists, limiting the communication and sharing of ideas and innovations. As such there is the need of resources and literature guides on the broad subjects involved that cut across the two groups.

At the invitation of the American Association of Physics Teachers a resource bibliography on plasma waves and instabilities was prepared and published in the American Journal of Physics [Grabbe, 1984a]. A selection of

classic benchmark papers and the bibliography were prepared and published in an associated book [Grabbe, 1986a]. This book will be of use to scientists in the fields of space plasmas, fusion and laboratory plasmas, and plasma device applications, as well as students of plasma physics.

REFERENCES

Akimoto, K., and N. Omidi, "The Generation of Broadband Electrostatic Noise by an Ion Beam in the Magnetotail", 13, 97 (1986).

Keith Balmain, "The Properties of Antennas in Plasmas," Annales des Telecommunications, 35, 273-283 (March-April, 1979).

Ashour-Abdalla, Maja, and H. Okuda, "Theory and Simulation of Broadband Electrostatic Noise in the Geomagnetic Tail," J. Geophys. Res. 91, 6833 (1986).

Dusenberry, Paul, "Convective Growth of Broadband Turbulence in the Plasma Sheet Boundary Layer," J. Geophys. Res. 92, 2560 (1987).

Eastman, Timothy, Louis Frank, and W. Peterson, "The Plasma Sheet Boundary Layer," J. Geophys. Res., 89, 1553 (1984).

Grabbe, Crockett, "Extraordinary Mode Resonance Cones in the Uranian Magnetosphere", J. Geophys. Res. 93, 14,309 (1988b).

Grabbe, Crockett, "Extraordinary Waves on the Resonance Cone Detected at Uranus," pp. 237-248 in H.O. Rucker, S.J. Bauer, and B.M. Pedersen (eds.) Planetary Radio Emissions II (Osterreichishcnen Akademie der Wissenschafter, Vienna, Austria, 1988a).

Grabbe, Crockett, "Generation of Broadband Electrostatic Noise in the Magnetotail with Two Electron Components," Proceedings of the International Conference on Plasma Physics, Luzanne, Switzerland (1984a).

Grabbe, Crockett, "Generation of Broadband Electrostatic Noise in the Magnetotail" in B. Buti (ed.) Advances in Space Plasma Physics (World Scientific, Singapore, 1985b).

Grabbe, Crockett, "New Results on the Generation of Broadband Electrostatic Noise in the Magnetotail", Geophys. Res. Lett. 12, 483 (1985a).

Grabbe, Crockett, "Numerical Study of the Spectrum of Broadband Electrostatic in the Magnetotail," J. Geophys. 92, 1185-1192 (1987a).

Grabbe, Crockett, Plasma Waves and Instabilities (American Association of Physics Teachers, New York, 1986a).

Grabbe, Crockett, "Pulse response from a small antenna in a magnetized plasma," University of Iowa Report (1986b).

Grabbe, Crockett, "Recent Developments on the Origin and Nature of Broadband Electrostatic Noise in the Plasma Sheet Boundary Layer." invited paper given at International Union of Radio Science XXIIth General Assembly in Tel Aviv, Israel (1987b).

Grabbe, Crockett, "Resonance cones and guided wave modes," Journal of

Plasma Physics, 24, 163-167 (1980).

Grabbe, Crockett, "Resonance Cones in Space Plasmas," invited paper at URSI conference at Boulder, Colorado (1989).

Grabbe, Crockett, "Resource letter: PWI-1 Plasma waves and instabilities," American Journal of Physics, 52, 970-981 (1984b).

Grabbe, Crockett, "Resonance cone structure in a warm, inhomogeneous, magnetized, bounded plasma with lower hybrid resonance layers," Journal of Plasma Physics, 33, 321-357 (1985d).

Grabbe, Crockett, "Review of the Generation of Broadband Electrostatic Waves in the Magnetotail," IEEE Trans. on Plasma Science 14, 902-909 (1986b).

Grabbe, Crockett, "Wave Propagation Effects on Ion Beam Modes in Broadband Electrostatic Noise in the Magnetotail," EOS 68 1439 (1987c).

Grabbe, Crockett and Timothy Eastman, "Generation of Broadband Electrostatic Noise by Ion Instabilities Beam in the Magnetotail", Journal of Geophysical Research 89, 3865-3872 and 3977-3982 (1984).

Grabbe, Crockett, and James Sheerin, "Langmuir turbulence in space plasmas," in Advances in Space Plasma Physics (World Scientific, Singapore, 1985).

Gurnett, Donald, Louis Frank, and Donald Lepping, "Plasma Waves in the Distant Magnetotail," J. Geophys. Res. 81, 6059-71 (1976).

Gurnett, Donald, William Kurth, Fred Scarf, and R. Poynter, "First Plasma Wave Observations at Uranus," Science 233, 106-109 (1986).

Hawegasa, Akira, Plasma Instabilities and Nonlinear Effects, No. 8 in Physics and Chemistry in Space series (Pergamon Press, New York, 1975), chapter 2.3.

James, H.G., "VLF Saucers", J. Geophys. Res. 18, 501-514 (1976).

Kennel, Charles and Maja Ashour-Abdalla, "Electrostatic Waves and the Strong Diffusion of Magnetospheric Electrons," chapter 5 in Atshiro Nishida (ed.) Magnetospheric Plasma Physics (D. Reidal Publishing, Boston, 1982).

Nishikawa, Kenneth, Louis Frank, Timothy Eastman, and Cheryl Huang, "Simulation of Electrostatic Turbulence in the Plasma Sheet Boundary Layer with Electron Currents and Ion Beams," in Anthony Lui (ed.) Magnetotail Physics (John Hopkins, Baltimore, 1987).

Mosier, Stephen, and Don Gurnett, "VLF Measurements of the Poynting Flux along the Geomagnetic Field with the Injun 5 Satellite," J. Geophys. Res. 74, 5675-5687 (1969).

T. Ohnuma, "Radiation Phenomenon of Plasma Waves," parts 1 and 2, IEEE Transactions of Plasma Science, 6, 464-504 (1978).

George Parks, M. McCarthy, R. Fitzenreiter, J. Etcheto, K. Anderson, Roger Anderson, Timothy Eastman, Louis Frank, Donald Gurnett, Cheryl Huang, R.

Lin, A. Lui, K. Ogilvie, A. Pedersen, H. Reme, and Donald Williams, "Particle and Field Characteristics of the High-Latitude Plasma Sheet Boundary Layer," J. Geophys. Res. 89, 8885-8906 (1984).

Reinleitner, Lee, Donald Gurnett, and Dennis Gallagher, "Chorus-related electrostatic bursts in the Earth's outer magnetosphere," Nature, 295, 46 (1982).

Reinleitner, Lee, Donald Gurnett, and Tim Eastman, "Electrostatic bursts generated by electrons in Landau resonance with whistler mode chorus, J. Geophys. Res., 88, 3079 (1983).

Schriver, David and Maja Ashour-Abdalla, "Generation of High frequency Broadband Electrostatic Noise: The Role of Cold Electrons," J. Geophys. Res. 92 5807 (1987).

APPENDICES: PUBLICATIONS SUPPORTED BY NASA GRANT NAGW-827

1. Grabbe, Crockett, and James Sheerin, "Langmuir turbulence in space plasmas," in Advances in Space Plasma Physics (World Scientific, Singapore, 1985).

2. Grabbe, Crockett, "Generation of Broadband Electrostatic Noise in the Magnetotail" in B. Buti (ed.) Advances in Space Plasma Physics (World Scientific, Singapore, 1985).

3. Grabbe, Crockett, "New Results on the Generation of Broadband Electrostatic Noise in the Magnetotail", Geophys. Res. Lett. 12, 483 (1985).

4. Grabbe, Crockett, "Resonance cone structure in a warm, inhomogeneous, magnetized, bounded plasma with lower hybrid resonance layers," Journal of Plasma Physics, 33, 321-357 (1985).

5. Grabbe, Crockett, "Pulse response from a small antenna in a magnetized plasma," University of Iowa Report (1986).

6. Grabbe, Crockett, Plasma Waves and Instabilities (American Association of Physics Teachers, New York, 1986).

7. Grabbe, Crockett, "Review of the Generation of Broadband Electrostatic Waves in the Magnetotail," IEEE Trans. on Plasma Science 14, 902-909 (1986).

8. Grabbe, Crockett, "Numerical Study of the Spectrum of Broadband Electrostatic in the Magnetotail," J. Geophys. 92, 1185-1192 (1987).

9. Grabbe, Crockett, "Recent Developments on the Origin and Nature of Broadband Electrostatic Noise in the Plasma Sheet Boundary Layer." invited paper presented at International Union of Radio Science XXIIth General Assembly in Tel Aviv, Israel (1987).

10. Grabbe, Crockett, "The Chemical Laser in a Ballistic Missile Defense", Amer. J. Phys. 56, 32 (1988).

11. Grabbe, Crockett, "Extraordinary Mode Resonance Cones in the Uranian Magnetosphere", J. Geophys. Res. 93, 14,309-15 and 14,733 (1988).

12. Grabbe, Crockett, "Extraordinary Waves on the Resonance Cone Detected at Uranus," pp. 237-248 in H.O. Rucker, S.J. Bauer, and B.M. Pedersen (eds.) Planetary Radio Emissions II (Osterreichishcnen Akademie der Wissenschafter, Vienna, Austria, 1988).

13. Grabbe, Crockett, "Resonance Cones in Space Plasmas," invited paper at presented at URSI conference at Boulder, Colorado (1989).

14. Grabbe, Crockett, "Wave Propagation Effects on Ion Beam Modes in Broadband Electrostatic Noise in the Magnetotail," accepted by J. Geophys. Res. (1989).

[Abstract in EOS 68 1439 (1987)].

15. Grabbe, Crockett, "The X-Ray Laser in Ballistic Missile Defense: I. The X-ray Laser and its Requirements", submitted to Eur. J. Phys., 1989.

16. Grabbe, Crockett, "The X-Ray Laser in Ballistic Missile Defense: II. Boost and Midcourse Defense", submitted to Eur. J. Phys., 1989.

H3-1 **RESONANCE CONES IN SPACE PLASMA**

Crockett L. Grabbe
Department of Physics
University of Iowa
Iowa City, IA 52242

Basic resonance cone theory and cases of occurrence of resonance cones in planetary magnetospheres are reviewed. Particular waveforms observed in the Uranian magnetosphere may also be generated by resonance cone phenomena, although the characteristics are different from known cases of resonance cone waves. Homogeneous theory suggests the sources are much closer to the spacecraft than the sources are for observations of saucers and auroral hiss. It is shown how effects of plasma inhomogeneities and temperature on the resonance cones can explain much of the fine structure of these waveforms.

APPENDIX 14

WAVE PROPAGATION EFFECTS OF BROADBAND ELECTROSTATIC NOISE IN THE MAGNETOTAIL

Crockett Grabbe

Department of Physics and Astronomy

University of Iowa

Iowa City, Iowa 52242

ABSTRACT

The theory for the generation of broadband electrostatic noise (BEN) by plasma instabilities of energetic ion beams that exist in the plasma sheet boundary layer (PSBL) predicts two characteristic signatures the wave data for BEN. These signatures are a gradual rise in the upper frequency of BEN as the spacecraft approaches the plasma boundary layer, and a very rapid rise in the upper frequency near the crossing into the plasma sheet boundary layer from the lobe. Wave data from the 1978 ISEE-1 mission is investigated during approaches and crossings for those 2 signatures. Several examples of crossings are presented that exhibit both signatures similar to that predicted by the theory. A case of crossings is shown in which the gradual frequency rise signature is absent but the rapid rise is present. This exhibits BEN in the range expected for the low frequency ion-ion 2-stream and the high-frequency Buneman instability. The intermediate frequencies are less intense, whfch may arise because the intermediate frequency beam-acoustic instability is close to stability (a warm beam temperature can quench it), as is the electron acoustic instability that can occur for warmer ion beams. An example is also given that was detected in a 1980 entry into the PSBL.

I. Introduction

Broadband electrostatic noise (BEN) in the magnetotail has recently been a major topic of experimental and theoretical research. BEN consists of a broad frequency band of incoherent waves running from 10 Hz to 10 kHz. Its generation region is known to be the boundary layer of the plasma sheet (PSBL), which plays an important role in the dynamics of the magnetotail. The PSBL is where energetic ion beams reside, where electron currents often occur, and where BEN (the most intense waves in the magnetotail) is generated. In addition, it is apparently a major transport region in the magnetotail [Eastman, et al. 1984; Grabbe and Eastman, 1984].

Observational evidence, showing a correlation of times of wave and particle occurrence, was presented in Grabbe and Eastman [1984] that BEN is generated by ion beam instabilities in the PSBL. A number of recent paper have focused on the development and analysis of the ion beam instability theory for the generation of BEN [Grabbe, 1984; 1985a,b; Omidi, 1985; Ashour-Abdalla and Okuda, 1986a,b; Akimoto and Omidi, 1986; Grabbe, 1986; 1987; Dusenberry, 1987; Shriver and Ashour-Abdalla, 1987; Nishikawa, et al., 1987; 1988].

Three instabilities of the ion beams that were shown to contribute to the spectrum of BEN in Grabbe [1985a,b and 1987]. These are: the ion acoustic instability on the beam, the Buneman instability (ion-electron two-stream instability) and the ion-ion two-stream instability. (The last instability was identified by Akimoto and Omidi [1986]). The beam-ion acoustic instability only occurs for cold ion beams (typically $\Delta v < 0.1\ v_b$, where Δv and v_b are the beam thermal and kinetic velocities), so may only be present at the edge of the PSBL.

Shriver and Ashour-Abdalla [1987] showed that the character of the instabilities can change as the beam temperature increases. In particular a fourth instability, the electron acoustic instability, may be responsible for generating the frequency band similar to that of the beam-acoustic instability when the ion beam temperature is sufficiently large to stabilize the latter [Ashour-Abdalla and Okuda, 1986b].

The ion acoustic instability is a negative energy mode instability in which an ion acoustic mode is on the ion beam propagating at a slower velocity than the beam. This instability generates the components at angles in a large cone centered about the magnetic field line. An analytical solution for the frequency and growth rate of that mode was given in Grabbe [1985b]. This instability tends to drive frequencies on the order of .01 f_{pe} to 0.1 f_{pe} unstable. Here f_{pe} is the plasma frequency, typically about 10 kHz. For higher temperature plasmas the electron acoustic instability tends to have a comparable frequency range [Ashour-Abdalla and Okuda, 1986b; Shriver and Ashour-Abdalla, 1987].

This ion-ion 2-stream instability occurs at a large angle to the magnetic field but for a narrow angular range. This instability generally has significantly larger growth rates than the ion acoustic instability, and generates lower frequencies (typically $f < .01\ f_{pe}$). It generates the lowest frequencies of BEN. For typical plasma sheet boundary conditions the angle of this instability is around 75 degrees, close to observations of this angle made to determine the polarization of the BEN spectrum at lower frequencies (100 Hz) in Gurnett and Frank [1976].

Analysis of the effect of the cold component of the electrons showed that they are responsible for producing the high frequency part

of the spectrum. The addition of only a 1% concentration of cold electrons can cause the upper frequency of the unstable waves to double and the growth rate of the high frequencies to substantially increase. The addition of cold electrons causes the ion acoustic instability to change and form a hybrid with the Buneman instability, so that higher frequencies become unstable and the cone of the instability about the magnetic field line narrows [Grabbe, 1987a]. As pointed out in Grabbe the most probable source of this population of electrons is diffusion from the lobe into the plasma sheet boundary layer, so the instability should be concentrated close to the interface between the boundary layer and the lobe. The presence of this component can explain why the unstable spectrum can extend to very near the plasma frequency, higher than can be produced by the hot components alone. This fact along with the concentration of this component along the field predicts a signature of a sudden rise of the BEN frequency to near the plasma frequency when the spacecraft enters the PSBL [Grabbe 1985a,b; 1986b; 1987a].

The ion beam instability theory makes predictions for the evolution of the observed waveforms as the spacecraft crosses from the lobe into the plasma sheet. In particular it predicts 2 signatures in the observed wave data for those crossings in which transitions can be identified. These signatures can be used to survey the data for evidence of the theory. As the spacecraft approaches the PSBL from the lobe the first waves from the ion beam instabilities it should detect are the large angle waves (θ ~ 70-75^{o}) from the ion-ion two-stream instabilit. Then the wave detector would begin picking the higher top frequencies of the ion and/or electron acoustic instabilities. The upper frequency of those instabilities rise as the maximum angle of propagation decrease,

so the top frequencies detected by the spacecraft gradually rise as the spacecraft approaches the boundary layer. This gradual rise in the wave frequency should be the first signature in these crossings.

A question that naturally arises about the ion-ion beam instability that has the large perpendicular propagation component is how far the wave can propagate into the lobe from its source in the PSBL. This depends on the Landau damping that it incurs. It should propagate out a few e-folding lengths $L = v_p/\gamma$, where v_p is its phase velocity and γ is the Landau damping rate. Neither v_p or γ have been determined for this mode for the conditions in the lobe. This question will be addressed in a future paper on the dispersion characteristics of the ion-ion beam instability.

Just seconds before crossing into the PSBL the spacecraft should detect the high frequencies generated by the Buneman instability near the plasma frequency. The waves generated by this instability are contained in a narrow cone along the magnetic field line, so these waves are confined to the vicinity of the PSBL (since the ion beams and the PSBL are approximately field-aligned). Once the spacecraft begins to detect the waves of this instability, it should very quickly detect waves in the complete frequency range of the instability. This sudden rise in the upper frequency of the BEN waves at the crossing into the PSBL is the second signature predicted by the ion beam instability theory on these crossings.

In Sec. II cases of the wave data for crossings of ISEE-1 into the PSBL will be examined for evidence of these 2 signatures. The concentration is on data detected in 1978, when the ion beams were generally more intense. A summary of the results is contained in Sec. III.

II. Comparison of Theoretical Predictions for BEN with Data

The 2 signatures predicted from the ion beam generation model for spacecraft crossings from the lobe into the PSBL are a rise in the top frequency cutoff of BEN as the spacecraft approaches the boundary layer from the lobe, and a rapid jump in that top frequency cutoff (to near the plasma frequency) as the spacecraft enters the boundary layer. The first signature is predicted because an ion-ion two-stream instability confined to large angles produces the lowest frequencies. As the spacecraft approaches the boundary layer it progressively detects the second instability, which is centered along the magnetic field line in a wide cone. The second signature because the Buneman instability, which occurs at the highest frequencies just below the plasma frequency, is confined in a narrow cone along the magnetic field line, and is not detected until the spacecraft is close to the boundary layer. There, all the high frequencies are seen very quickly.

An analysis of data gathered from the ISEE-1 spacecraft crossing from the lobe to the boundary layer is made to find cases for the signatures predicted from the theoretical model, and to also search for cases where the signatures may be absent. This data may provide supporting evidence for the theoretical model of the origin of BEN waves that has been developed in several recent papers.

The time of the spacecraft entry into the boundary of the plasma sheet from the lobe can be identified from the particle data. At the time of the entry the electron temperature rises dramatically, and this appears in the data as a sudden appearance of energetic electrons at a continuous range of energies up to about 100 - 200 eV. (When the spacecraft is in the lobe the low temperature electrons are completely masked

by the photoelectrons in the instrument.) This data has been used to provide specific times of entry to use in the wave data analysis.

In Plate 1 is an example of the evolution of the wave data with the characteristic signatures similar to that predicted by the theory of these instabilities both on an exit from the PSBL into the lobe and on the entrance into the PSBL from the lobe. The spacecraft first exits the PSBL to the lobe at 0110 UT on day 048 of 1978 at a distance of just over 13 R_E. It then re-enters the PSBL from the lobe at 0225 UT at a distance of just over 14 R_E. The drop and rise of the frequency maximum forms almost a mirror image. As the spacecraft leaves the plasma sheet the upper frequency with a yellow intensity drops down quite rapidly (about a minute or two) from 2 - 3 kHz to 0.7 - 0.8 kHz. It then drops more gradually, going below 0.1 kHz at about 0135 UT. It then begins to rise again, going above 0.1 kHz again at about 0150 UT, as the spacecraft approaches the plasma sheet again. It rises gradually to about 0.8 kHz just before 0225 UT, then jumps quickly up to near 4 kHz at the time. Both signatures predicted by the theory are observed both on the exit and the re-entrance into the PSBL.

For the wave data in Plate 2 the ISEE-1 spacecraft is approaching the plasma sheet from the lobe at a distance from the Earth around 21 R_E, and at a time of around 0300 UT of day 085 of 1978. The wave spectrum is first seen at time 0250 UT, when the spacecraft is still well in the lobe. BEN ranging up to about 200 Hz is detected at that time, and it rises to a yellow intensity about 0290 UT. The data shows a gradual rise in the maximum frequency of yellow intensity to about 600 Hz at about 0320 UT the upper frequency begins rising rapidly, and at 0323 UT a dramatic jump in the upper frequency to about 6 kHz occurs. This is

the spacecraft enters the plasma sheet boundary layer from the lobe at 0324 UT. Again, both of the signatures predicted by the theory are clearly seen in this case, with the first (gradual rise) signature being quite prominent in the case.

In the wave data gathered in Plate 3 the spacecraft enters the PSBL from the lobe at 1952 UT on day 154 of 1978, at a distance of just under 17 R_E. At about 1935 UT it detects the lower frequencies of yellow intensity BEN up to about 150 Hz, and the upper frequency rises, reaching about 800 Hz at around 1945 UT. Shortly afterward, at about 1950 UT, the upper frequency rises at a much faster rate, reaching 3 kHz by the entry into the PSBL. This case also exhibits both signatures predicted by the theory on the entrance into the PSBL.

In the wave data of Plate 4 the spacecraft enters the PSBL at 0357 UT on day 060 of 1978, at a distance of just under 17 R_E. Although chorus waves were present at previous times, the first detection of BEN above 100 Hz occurs about 0342 UT. The upper frequency of yellow intensity rises to about 600 Hz around 0355 UT. Then it rises much faster, reaching about 3 kHz on the entry into the PSBL. Although the first signature is not as prominent as in Fig. 2, this case shows both characteristic signatures predicted from the ion beam instability theory.

In Plate 5 is a case observed on ISEE-1 spacecraft where 1 of the 2 signatures was absent on a PSBL crossing. This was taken on Day 133 of 1978. The spacecraft entered the plasma sheet just before 1000 UT, at a distance of just under 15 R_E. BEN is first detected (at the yellow intensity) just before 0950 UT. There is no signature of a continuous rise in the upper frequency of BEN for the few minutes after that time. Then just before 1000 UT there is the sudden appearance of high frequen-

cies around 1 kHz and above. This high frequency sudden appearance is apparently a scaled-down version of the second signature. This scaling down plus the absence of the first signature seems to arise because of the relative stability of the central frequencies of BEN. This would correspond to the ion and/or electron acoustic instability having a low growth rate, whereas the low frequency ion-ion streaming instability and the high frequency Buneman-type instability are more unstable.

In the numerical calculations in Grabbe [1985a,b; 1987] it was shown that for the low-temperature ion beams analyzed the growth rate of the low frequency instability was much larger than for the central frequency ion beam acoustic instability. Furthermore, the presence of only 1% cold electrons makes the higher frequencies unstable, growing at a rate much larger than the central frequencies. As the temperature of the ion beams increases the growth rate of the central frequencies from the ion acoustic instability decrease. Thus is would be expected that in some cases the central frequency intensity would be subdued. Thus the BEN data in Plate 5 is well explained by the theory of the ion beam instabilities, and provides evidence that 3 instabilities are present.

The above cases all occurred in the ISEE-1 data taken in the magnetotail in 1978. This is because the ion beams and BEN were very prominent during the period which that data was taken. The ISEE-1 spacecraft also gathered data in the magnetotail during 1980, when the ion beams were considerably less intense, and BEN is similarly less prominent. It is more difficult to see the characteristic signatures in that data, but they are present at times.

As an example, Plate 6 contains the wave data recorded on Day 084 of 1980. The spacecraft enters the PSBL from the lobe about 0323 UT.

It starts detecting more intense BEN around 0310 UT. There is no clear signature of a rise in the upper frequency of BEN, although the intensity of some of the higher frequencies increases closer to the PSBL. Then just before the spacecraft enters the PSBL the highest frequencies of the spectrum appear at the yellow intensity quite suddenly, with a rapid frequency rise. This is the second signature of predicted by the ion beam instability theory.

III. Summary

An analysis of the wave and particle data from ISEE-1 for 1978 yielded several example of crossings between the lobe and the PSBL which exhibited the signatures predicted by theoretical analyses of generation of BEN by ion beam instabilities. One case also showed both signatures on the spacecraft exit from the PSBL to the lobe, and another showed a clear lack of one of the signatures, with an interesting spectrum.

The unusual spectrum observed on day 133 of 1978 with a signature absent can be explained as being a case where the instability (ion or electron acoustic) that generates the central frequencies of the spectrum as being subdued -- the ion beam temperature and plasma conditions caused the ion and/or electron acoustic mode to be close to stability. The low frequency ion/ion 2-stream instability is first detected as the spacecraft approaches the lobe, but no upper rising frequency is detected because the middle frequency is not detected. Upon crossing into the PSBL the high frequency Buneman instability is detected, and the central frequencies are detected at a much lower intensity.

It is hoped this comparison of the ion instability signatures predicted from the theory with the wave data will stimulate other comparisons of the theory and the data. One prediction of the ion beam instability theory is that the nature of the source continually varies over the plasma sheet boundary layer. Right at the interface of the boundary layer with the lobe diffusion of cold electrons indirectly inferred to be there. This creates the very high part of the spectrum near the plasma frequency through the positive energy Buneman instability. In this case the large angle mode is more stable.

Outside of this diffusion region the cold electrons are negligible

and the spectrum is similar to that analyzed for the one electron model. There the strong instability at the large angle occurs and generates the prominent features of the lower frequency part of the spectrum. In this case the frequencies right below the plasma frequency tends to be stable. The ion-ion 2 stream instability is unstable and produces the lower frequencies of the spectrum. However, the ion beam gets hotter (as shown in Eastman [1984] and Grabbe and Eastman [1984]]) and at some point the ion acoustic instability stabilizes. Past this point (deeper in the PSBL) the upper frequencies are produced by the electron acoustic instability. This predicted evolution may cause other features in the wave data in addition to the 2 signatures investigated in this paper.

ACKNOWLEDGMENTS

I would like to thank Tim Eastman for discussions on the particle data taken simultaneous to the wave data in this paper.

This research was supported in by grants NAGW-827 and NAG5-1093 with the National Aeronautics and Space Association, and a grant with the National Science Foundation.

REFERENCES

Akimoto, K., and N. Omidi, "The generation of broadband electrostatic noise by an ion beam in the magnetotail," Geophys. Res. Lett., 13, 97, 1986.

Ashour-Abdalla, M., and H. Okuda, "Theory and simulation of broadband electrostatic noise in the geomagnetic tail," J. Geophys. Res., 91, 6833, 1986a).

Ashour-Abdalla, M., and H. Okuda, "Electron acoustic instabilities in the geomagnetic tail," Geophys. Res. Lett., 13, 366, 1986b.

Dusenberry, P., "Convective growth of broadband turbulence in the plasma sheet boundary layer," J. Geophys. Res., 92, 2560, 1987.

Eastman, T. E., L. A. Frank, W. K. Peterson and W. Lennartsson, "The plasma sheet boundary layer," J. Geophys. Res., 89, 1553, 1984.

Grabbe, C. L., "Generation of broadband electrostatic noise in the magnetotail with two electron components," Proceedings of the International Conference on Plasma Physics, Luzanne, Switzerland (1984).

Grabbe, C. L., "Generation of broadband electrostatic noise in the magnetotail" in B. Buti (ed.) Advances in Plasma Physics (World Scientific, Singapore, 1985b).

Grabbe, C. L., "New results on the generation of broadband electrostatic noise in the magnetotail", Geophys. Res. Lett., 12, 483, 1985a.

Grabbe, C. L., "Numerical study of the spectrum of broadband electrostatic in the magnetotail," J. Geophys., 92, 1185-1192, 1987a.

Grabbe, C. L., Plasma Waves and Instabilities (American Association of Physics Teachers, College Park, MD, 1986a).

Grabbe, C. L., "Recent developments on the origin and nature of broadband electrostatic noise in the plasma sheet boundary layer." invited paper given at International Union of Radio Science XXIIth General Assembly in Tel Aviv, Israel, 1987b.

Grabbe, C. L., "Review of the generation of broadband electrostatic waves in the magnetotail," IEEE Trans. on Plasma Science, 14, 902-909, 1986b.

Grabbe, C. L. and T. E. Eastman, "Generation of broadband electrostatic noise by ion instabilities beam in the magnetotail", Journal of Geophysical Research, 89, 3865-3872 and 3977-3982, 1984.

Gurnett, D., L. A. Frank, and D. Lepping, "Plasma waves in the distant magnetotail," J. Geophys. Res., 81, 6059-71, 1976.

Marsch, E., "Beam-driven electron acoustic waves upstream of the

Earth's bow shock," J. Geophys. Res., 90, 6327-6336, 1985.

Nishikawa, K.-I., L. A. Frank, T. E. Eastman, and C. Y. Huang, "Simulation of electrostatic turbulence in the plasma sheet boundary layer with electron currents and ion beams," in Anthony Lui (ed.) Magnetotail Physics (John Hopkins, Baltimore, 1987).

Nishikawa, K.-I., L. A. Frank, and C. Y. Huang, "Simulation of electrostatic turbulence in the plasma sheet boundary layer with electron currents and bean-shaped ion beams," J. Geophys. Res., 93, 5929-35, 1988.

Omidi, N., "Broadband electrostatic noise produced by ion beams in the Earth's magnetotail", J. Geophys. Res., 90, 12330, 1985.

G. Parks, M. McCarthy, R. Fitzenreiter, J. Etcheto, K. Anderson, R. R. Anderson, T. E. Eastman, L. A. Frank, D. Gurnett, C. Y. Huang, R. Lin, A. Lui, K. Ogilvie, A. Pedersen, H. Reme, and D. Williams, "Particle and field characteristics of the high-latitude plasma sheet boundary layer," J. Geophys. Res., 89, 8885-8906, 1984.

Schriver, D. and M. Ashour-Abdalla, "Generation of high frequency broadband electrostatic noise: The role of cold electrons," J. Geophys. Res., 92, 5807, 1987.

FIGURE CAPTIONS

Plate 1. Sweep Frequency Receiver (SFR) wave data from ISEE-1 for day 048 of 1978 for 0000 to 0600 UT. The spacecraft first exits the PSBL to the lobe at 0110 UT, then re-enters the PSBL from the lobe at 0225 UT. As the spacecraft leaves the plasma sheet the upper frequency drop down quite rapidly at first, then drops more gradually, Then it begins to rise again, as the spacecraft approaches the plasma sheet again. Both signatures predicted by the theory are observed both on the exit and the re-entrance into the PSBL.

Plate 2. SFR wave data for day 085 of 1978 for 0000 to 0600 UT. The spacecraft enters the plasma sheet boundary level about 0323 to 0324 UT, and the broadband electrostatic noise before and during this time exhibits signatures predicted by the theory. The signature of the gradual rise in frequency as the spacecraft approaches the plasma sheet is particularly good for this case. [After Grabbe and Eastman, 1984].

Plate 3. SFR data for day 154 of 1978. The spacecraft enters the PSBL from the lobe at 1952 UT. At about 1935 UT it detects the lower frequencies of BEN up to about 150 Hz, and the upper frequency rises, reaching about 800 Hz at around 1945 UT. At 1950 UT, the upper frequency rises at a much faster rate, reaching 3 kHz by the entry into the PSBL. This case also exhibits both signatures predicted by theory.

Plate 4. SFR data for day 060 of 1978. The spacecraft enters the PSBL at 0357 UT. The first detection of BEN above 100 Hz occurs about 0342

UT, with chorus waves being present at previous times. The upper frequency of BEN rises to about 600 Hz around 0355 UT, then reaches about 3 kHz on the entry into the PSBL. This case exhibits both signatures.

Plate 5. SFR data taken on Day 133 of 1978. The spacecraft enter the PSBL about 1000 UT. BEN is first detected just before 0950 UT, but no signature of a continuous gradual rise in the upper frequency of BEN occurs. that time. Just before 1000 UT is the sudden appearance of high frequencies around 1 kHz and above, which exhibits the second signature. This arises because of the relative stability of the central frequencies of BEN. The ion and/or electron acoustic instability is more stable than the low frequency ion-ion streaming instability and the high frequency Buneman-type instability.

Plate 6. SFR wave data recorded on Day 084 of 1980. The spacecraft enters the PSBL from the lobe about 0323 UT. It starts detecting more intense BEN around 0310 UT. The first signature is of the gradual rise of the frequency is not present. Just before the spacecraft enters the PSBL the highest frequencies of the spectrum appear rather, which is the second signature of predicted by the ion beam instability theory.

APPENDIX 15

PHYSICS OF THE X-RAY LASER IN A SPACE-BASED BALLISTIC MISSILE DEFENSE

I. The X-ray Laser and Its Requirements

Crockett Grabbe

Department of Physics

University of Iowa

Iowa City, Iowa 52242

ABSTRACT

The basic physics of the X-ray laser driven by a nuclear explosion and its proposed uses in a space-based ballistic missile defense are analyzed in this and a following paper. This paper concentrates on the physics of the X-ray lasing device and conditions that must be achieved. The basic physical mechanisms on which it is based are summarized. The laser gain achievable, conditions for achieving a desired efficiency, and strength of the bomb required are calculated. The penetration depths of the X-ray beam and a possible countermeasure to its use as a defensive weapon are surveyed. The minimum strength of the nuclear blast and the angular concentration of energy required from the laser are determined.

I. Introduction

One system being investigated as a possible defense against ballistic missiles under the Strategic Defense Initiative of the US is the X-ray laser powered by a nuclear explosion. While most of the research on this device is classified, the basic physics of such a system and its major strengths and weaknesses as a defensive weapon can be analyzed.

To achieve the intensities of radiation desired at these short wavelengths requires a very large power source. The prodigious amount needed can be attained in a nuclear explosion, which serves as the pump. (See Figure 1.) The explosion destroys the defense system, so the power must be generated in the very short time between the ignition of the explosion and the disintegration of the laser structure (less than 10^{-8} seconds).

An analysis of the requirements of this laser weapon using physics principles will be made in this paper. Physical requirements and limitations for its proposed defensive uses, as well as possible implications it has for arms control, will be presented in a following paper (II).

II. How the X-ray Laser Works

At X-ray wavelengths there are no mirrors or coherent reflectors available, so the laser does not utilize feedback or cavity resonators. Thus the X-ray is not sharply focused but emerges in a cone whose angular spread is determined by the geometric properties of the source, which acts as a plasma lens for the X-rays.

The laser is composed of a number of rods consisting of fibers surrounded by diffuse lead reflectors (see Figure 1). The nuclear explosion sends out high-energy X-rays and gamma rays, a portion of which enter the rods and strip the electrons out of atoms in the fiber, producing highly ionized ions. At the high temperatures present in the nuclear explosion (10^8 ^oK) on average only a single electron remains bound in the electron shells of the atom, so the hydrogenic ions constitute the rods.

Certain hydrogenic ions have metastable (long-lived) excited energy levels that the electron can occupy. Such ions are candidates for use in the fiber since they provide a means for achieving a population inversion: the electrons stay in this metastable state for a time (10^{-13} sec. in zinc) but when they decay to the next lower state, they stay in this lower state for a much briefer period of time (10^{-15} sec. in zinc), quickly decaying to an even lower state. Thus, on average there are more atoms with electrons in the metastable state than in the lower state that the electron first decays to. The goal is to find atoms whose hydrogenic ions have good metastable excited states (Bunkin et al. 1981, Robinson 1984, Ritson 1987).

One can understand how X-ray frequencies f are achieved by looking at the energy levels the bound electron can occupy in the hydrogenic ion. Their difference would be the energy emitted E (directly proportional to the frequency) for a transition to from orbital level n_1 to n_2. This is the same as for a normal hydrogen ion, except the atomic number Z (number of protons) of the atom used for the laser:

$$E(n_2,n_1) = (Z^2 m_e e^4/2h^2)(1/n_1^2 - 1/n_2^2)$$

$$= 13.6 \text{ eV } Z^2(1/n_1^2 - 1/n_2^2) \qquad (1)$$

$$= hf$$

where h is the familiar Planck's constant, m_e the electron mass, e the charge of the electron, and f the frequency of the emitted radiation. If an atom with Z ~ 30 or more is used the frequency is large enough to lie in the X-ray range.

The idea of using metastable transitions in hydrogenic ions for an X-ray laser has been investigated for some time. Chapline and Wood, for example, discuss this process and possible power sources, such as cooling on very short time scales (requiring 10^{15} watts) and resonant charge exchange (requiring 10^{12} watts). They mention, for example, that hydrogenic krypton could be pumped from its n = 1 ground state to its n = 3 metastable excited state with 15.7 keV of pumping energy, and lase at 2.5 keV when it decays down to the n = 2 state (decaying much faster then to the n = 1 state), producing soft X-rays (Chapline and Wood, 1975).

What is new with the development of an X-ray laser for a ballistic missile defense is the use of a nuclear explosion to provide a very large power source for the laser, in an effort to develop a very powerful laser beam needed for these applications. Among the first to investigate the basic elements of this scheme were some Soviet physicists, who identified the metastable states of zinc or copper as appropriate for an X-ray laser (Bunkin et al. 1981). Lasers using these metals would lase at a wavelength λ of around 14 A.

X-ray laser experiments have been performed at Lawrence Livermore Laboratory and the Princeton Plasma Physics Laboratory which have shown that large gains can be achieved by selenium fibers, and somewhat

smaller but significant gains can be achieved by carbon. These latter elements lase at longer wavelengths in a range that is called the extreme ultraviolet (on the borderline to the X-ray range.) Later reports indicate the Lawrence Livermore measurements were probably in error, but there is little doubt that lasing has occurring in these experiments (Smith 1985).

The following sections develop the requirements for an X-ray laser used for a defense. Recent publications have addressed aspects of the physics of an X-ray laser as well (Ritson 1987, Tsipis 1985, Velikhov et al. 1986).

III. The X-ray Laser Gain Achievable

One can determine how much more intense the X-rays that hit the missile will be with the X-ray laser than for a normal nuclear explosion. The X-ray laser directs part of the energy of the nuclear blast in a small angular range, while a normal nuclear explosion causes the energy to spread out uniformly in a sphere (see Fig. 2). Thus the energy density that is achieved at the missiles is (Drell et al. 1985):

$$U = \frac{E_{bomb}}{4\pi r^2} \cdot \frac{4\pi\epsilon}{\pi(\theta/2)^2} = \frac{4\epsilon E_{bomb}}{\pi\theta^2 r^2} \qquad (2)$$

Here r is the distance of the missile from the nuclear X-ray laser explosion, ϵ is the efficiency of the laser, and E_{bomb} is the explosive energy of the nuclear device.

The first factor in Eq. (2) for U is just the spreading of the energy density of the nuclear explosion, and the second term is the laser gain G due to the concentration to a small angle θ. The second term contains the ratio of the full solid angle to the small solid angle of the laser beam. We have neglected the part of the bomb's energy that goes into expansion, kinetic energy, and lower frequencies of radiation, including heat (infrared) radiation. However, most of the energy will go into the X-ray and gamma ray frequencies which can contribute to the laser (Glasstone and Dolan 1977).

The angle of divergence θ depends on 2 quantities: the diffraction-limit angle $1.22\ \lambda/d$ and the geometry divergence angle d/L cause by the finite length L laser fibers, where d is the is the diameter of the laser fibers. The total angle is given by

$$\theta = [(1.22\ \lambda/d)^2 + (d/L)^2]^{1/2} \qquad (3)$$

d would be chosen to achieve the minimum angle of divergence. This can be easily determined by a variational principle, where the derivative of θ with respect to d is set equal to 0. This yields values for the minimum d and θ (Walbridge 1984):

$$d_{min} = (1.22\ \lambda L)^{1/2} \qquad (4)$$
$$\theta_{min} = (2.44\ \lambda/L)^{1/2}$$

One can now calculate a typical example of for these numbers. λ is set equal to 14 A as used above, and L will be chosen to be 3 m. We then have

$$d_{min} = 71.6\ \mu m$$

$$\theta_{min} = 3.37 \times 10^{-5} \text{ radians} \qquad (5)$$

G can be determined for the case that the column is tailored in the manner to minimize the angle of divergence. One must also know the efficiency of conversion from the energy of the nuclear blast to the X-ray laser, and this will be assumed to be 1%. (The laser conditions necessary to achieve this efficiency are discussed in the appendix). From equation (2), the gain is then:

$$G = 16\epsilon/\pi\theta^2 = 0.45 \times 10^8 \qquad (6)$$

G represents the huge increase in the amplitude of the X-ray radiation at this wavelength because of the X-ray laser, being the increase of the energy intensity of X-rays over that produced by an ordinary nuclear explosion.

The gain of the laser comes about because part of the bomb power is highly directional. This allows for much higher intensities away from the bomb, which would be needed to kill missiles (and other targets). Because of the enormous increase in the destructive energy available from these and similar devices of that of a simple nuclear explosion, they have become known as third generation nuclear weapons (Tsipis, 1986). (The atomic bomb was the first generation and the hydrogen bomb the second generation.)

IV. Laser Energy Required to Kill Missiles

Estimates have been made that show the energy density necessary to kill a hardened missile in the boost phase to be about 20 kj/cm^2 (Gottfried et al. 1984, Carter 1984). In the following paper (II) the distances the x-ray laser beam has to travel to reach the boosters is calculated for three locations of the missile fields. The x-ray laser beam must be sufficiently strong to destroy the missiles at this greatest distance.

If W is the energy of the nuclear explosion, and r is the distance to beam has to go to hit the missiles, then the basic requirement for destroying the missiles is that the energy intensity of the X-ray laser at the missiles exceeds the minimum required to kill the missile:

$$GW/4\pi r^2 = 20 \text{ kj/cm}^2. \qquad (7)$$

The maximum distance r determined in part II that the laser beam has to travel for a boost-phase defense against missiles further north in the Soviet Union is 4,949 km. For this and the least angle gain of equation (6), the explosive force is then

$$W = (\pi^2 r^2 \theta^2/4\epsilon)(20 \text{ kJ/cm}^2) = 1.37 \text{ X } 10^{15} \text{ J} = 343 \text{ kilotons} \qquad (8)$$

In general, it may not be possible to achieve the minimum divergence angle, or it may even be necessary to enlarge it to ensure that all the missiles are in its path. The necessary energy in the nuclear explosion is often expressed per steradian of the solid angle:

$$W \times [1 \text{ steradian}/\pi(\theta/2)^2] = 1.5 \times 10^{24} \text{ J/steradian} \quad (9)$$

For a 2,000 km range of destruction, this value gets reduced by a factor of 6. This is slightly larger than the intensity set by the Fletcher panel (which assumed a 2,000 km range) of 10^{22} j/steradian as the goal in the development of an x-ray laser. It is also slightly greater than that estimated by Hafemeister (Robinson 1983, Hafemeister 1984).

V. The Absorption of X-rays at a Target

The intense X-rays produced by the laser are absorbed in a thin surface of an object attacked by the rays. Several processes affect the absorption of the X-rays, but for the energy at which the X-ray laser would operate (near 1 keV), the absorption is dominated by the photo-electric effect. This causes the penetration distance of the X-rays to be very short.

The intensity of the X-ray beam of initial intensity I_o is given by:

$$I = I_o \exp(-\mu x) = I_o \exp[-(\mu/\rho)\rho x] \quad (10)$$

where μ is the absorption coefficient of the X-rays and ρ is the mass density. (μ/ρ) can be found from tables. There are several sources that gives values for X-rays above 10 keV (Gray 1972, Evans 1955), and extrapolation can give a rough estimate for lower values.

In table 1 values of (μ/ρ) of metals that would be used in a

missile are given from a source with 1 keV energies (McMaster 1969). Also given are the density ρ and the e-folding penetration length $1/\mu$. They show that the energy of the X-ray laser gets absorbed in a fraction of a micron from the surface of the missile, in agreement with Bethe who estimate the depth at 0.1 micron for Fe and Ni at 1 keV (Gottfried et al., 1984)!

This very thin surface absorption of the intense X-ray energy causes the surface of the missile to explode, damaging what is underneath through one of 2 processes. The first process is by just crushing what is underneath from the force of the impact. The second process involves damage from nuclear reactions induced by the high energy of the shock from the skin (called spallation), which causes ejection of neutrons and protons from the nucleus of the inner skin (Garwin and Bethe 1968).

This has several consequences. One is that the X-ray laser is especially attractive for use in the midcourse for destroying the balloon decoys that would be used to hide the re-entry vehicles (if a missile defense is present). The balloons are thin-surfaced, and the X-ray energy is almost completely absorbed in this surface. This totally explodes the balloon, exposing the warhead it may contain.

A second consequence of quick surface absorption of X-rays is that they cannot penetrate very far into the atmosphere. For the atmosphere as well, the photoelectric effect dominates in the absorption (and over effects such as Rayleigh scattering). The density of the atmosphere varies with height. From Evans (1955) or Gray (1972), making an extrapolation of (μ/ρ) for air to 1 keV one finds $(\mu/\rho) = 6.7 \times 10^3$ cm^2/g.[13] The density of air at 100 km altitude is $\rho = 5.60 \times 10^{-10}$

Table 1:

Penetration Lengths of 1 keV X-rays (λ = 12.5 A) for Booster Metals

Metal	μ/ρ (cm^2/g)	ρ (g/cm^3)	$1/\mu$ (μm)
Iron	9.32×10^3	7.86	0.136
Nickel	1.05×10^4	8.90	0.108
Aluminum	1.18×10^3	2.70	3.15

g/cm^3 (Fleagle and Businger, 1980). Thus the vertical penetration distance is then:

$$1/\mu = 2.67 \text{ km}. \tag{11}$$

Modelling the variation of the air density with height from the table in Fleagle and Businger we find that about 90% of the intensity of the X-ray beam is absorbed when it reaches 100 km altitude (using vertical penetration).

This short penetration depth implies the X-rays could not be used to counter missiles in the atmosphere, at heights of about 100 km or below. The defense must wait until the missiles have left the atmosphere before it can attack them, and the X-ray laser beam must stay above this level.

A third consequence is that a countermeasure of shielding could be devised to protect the missiles and warheads against the X-ray laser beam. This would be to put a false surface on the target, as shown in Figure 2. The false surface would be a very thin metallic surface (thickness ~ 1 μm) to absorb the X-rays and explode. Underneath this surface a cushion could be made that separated it from the inner surface. This cushion would be designed to absorb the impact force of the explosion caused by the X-ray laser beam, protecting the inner surface.

This layer of protection may only protect against the firing of one X-ray laser, but multiple false surface and multiple shields could protect against multiple firings. However, in return for installing a shield or shields, greater weight is added to the missile or its warheads. This limits the payload that is available for the missile

unless a new line of boosters is designed with larger fuel tanks. The false surface will be very thin, adding almost no weight to what it is shielding. If the shock absorbing layer was made of crushable foam or other lightweight materials, the weight addition would not be significant, either. Such materials would have to be tested to develop the shield.

ACKNOWLEDGMENTS

I would like to thank Harvey Lynch of Stanford University for his helpful comments on the paper.

This work was supported in part by the National Aeronautics and Space Administration of the United States.

APPENDIX: Requirements for 1% efficiency of the X-ray Laser

What are the requirements in the X-ray laser weapon for achieving the 1% efficiency assumed in the text? The efficiency is equal to the ratio of the X-ray laser energy and the energy of the explosion:

$$\epsilon = U_{xrl}/U_{exp} \tag{A1}$$

U_{xrl} obtainable must be determined from the design.

The X-ray laser energy can be determined as follows: the energy of radiation emitted by the electron transition in each ion in the lasing rods U_{trans} is multipled by the number of atoms in the rod N_{atm}, which is then multiplied by the number of times each atom recycles this release of laser radiation N_{rec} (on the average) and the number of rods N_{rod} in the laser. N_{atm} is then easily determined from the mass density of the rod ρ, the volume of the rod $\pi Ld^2/4$ (where L is the rod length and d its diameter as determined in Section III), and the atomic mass A multipled by the proton mass m_p. This gives us a general equation for the efficiency:

$$\epsilon = \pi d^2 L N_{rod} N_{rec} U_{trans}/4 m_p A U_{exp} \tag{A2}$$

This equation is only valid for efficiencies $\epsilon << 1$, since as approaches 1, the rods are strongly competing with each other for the available energy, reducing the right hand side of the equation.

An example of the conditions necessary to achieve a certain efficiency is can be easily done. Assume the lasing rod is made of

zinc. The transition energy is then[9]:

$$U_{trans} = 0.9 \text{ keV} = 1.44 \text{ X } 10^{-12} \text{ ergs.} \qquad \text{(A3)}$$

Other parameters are constants for zinc or representative values from constraints derived in the text:

$$A = 65.4 \qquad \rho = 7.13 \text{ g/cm}^3 \qquad \text{(A4)}$$

$$m_p = 1.67 \text{ X } 10^{-13} \qquad U_{exp} = 100 \text{ ktons}$$

These give:

$$\epsilon = (2.84 \text{ X } 10^{-9}) N_{rod} N_{rec} \qquad \text{(A5)}$$

The number of rods and the number of recyclings of the electron into the upper state in the ion determines ϵ. Since the transition time for the zinc ion is about 10^{-13} seconds, while the rods last about 10^{-9} seconds before the blast destroys them, then the maximum N_{rec} can be is about 10^4. This means that a minimum of number of rods of about 400 is required to surround the explosion to get a 1% efficiency in the blast. N_{rec} may be significantly smaller (possibly as small as 1), so N_{rod} will have to be correspondingly larger.

REFERENCES

Bunkin F V, Dershiev V I, and Yakovlenko S I 1981 Sov. J. Quantum Electron. **11** 971

Carter A 1984 Directed Energy Missile Defense in Space (Washington, DC: Office of Technology Assessment).

Chapline G and Wood L, 1975 Phys. Today **28** 40.

Drell S, Farley P, and Holloway D 1985 The Reagan Strategic Defense Initiative (Cambridge, Massachusetts: Ballinger).

Evans R 1955 The Atomic Nucleus (New York: McGraw-Hill) chap. 25.

Fleagle R and Businger J 1980 An Introduction to Atmospheric Physics (New York: Academic Press) Appendix IIE.

Garwin R and Bethe H 1968 Scient. Amer. **219** 21.

Glasstone S and Dolan P 1977 The Effects of Nuclear Weapons (Washington, DC: Government Printing Office)

Gottfried K, Kendall H, Bethe H, Clausen P, Garwin R, Gaylor N, Lebow R, Sagan C, and Weisskopf V 1984 Space-Based Missile Defense (Cambridge, Massachusetts: Union of Concerned Scientists) Technical Appendix.

Gray D (Ed.) 1972 American Inistute of Physics Handbook Third Edition (New York: McGraw-Hill) sec. 8e

Hafemeister D 1984 SPIE (IEEE) **474** 100

McMaster W H 1969 Lawrence Livermore Laboratory Report UCRL-50174.

Ritson D M 1987 (Aug. 6) Nature **328** 487

Robinson A L 1984 Science **226**, 821

Robinson C 1983 (Oct. 24) Aviation Week and Space Technology **119**, 50

Smith R J 1985 Science **230** 646

Tsipis K 1986 chap. 3 in Stockholm International Peace Researh Institute Yearbook 1985 World Armaments and Disarmament (Oxford: Oxford University Press).

Velikhov Y, Sagdeev R, and Kokoshin A 1986 Weaponry in Space: The Dilemna of Security (Moscow: MIR Publishers)

Walbridge E Weapons 1984 (July 19) Nature **310** 180

FIGURE CAPTIONS

Figure 1. Basic components of the X-ray laser.

Figure 2. Countermeasure of protecting a missile against an X-ray laser. The outer false surface is designed from metals and is only about 1 micron thick. The cushion absorbs the impact of the explosion to protect the inner surface. These features are grossly exaggerated in size in the picture.

A-G86-364-I

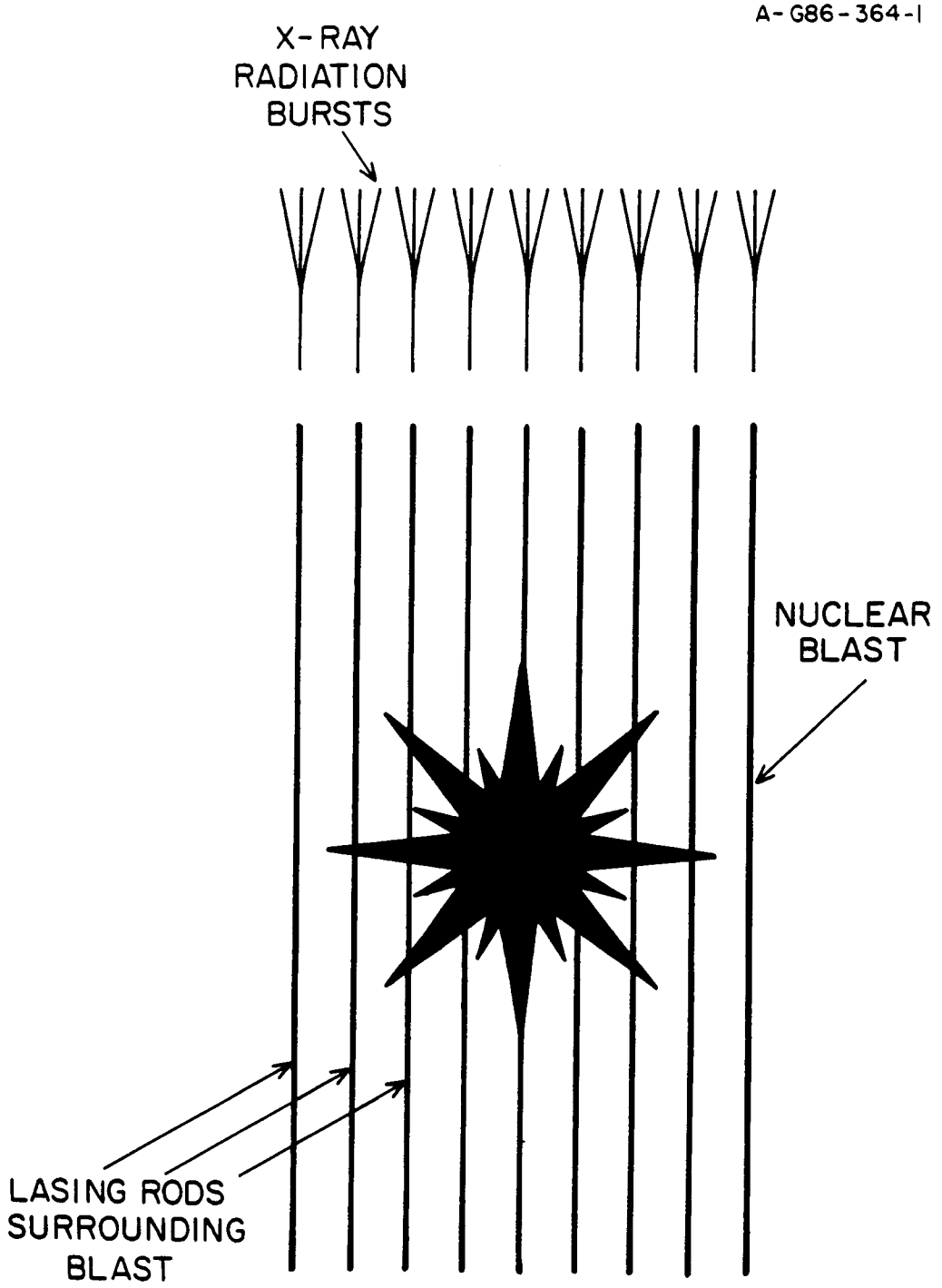

X-RAY LASER

A-G87-541

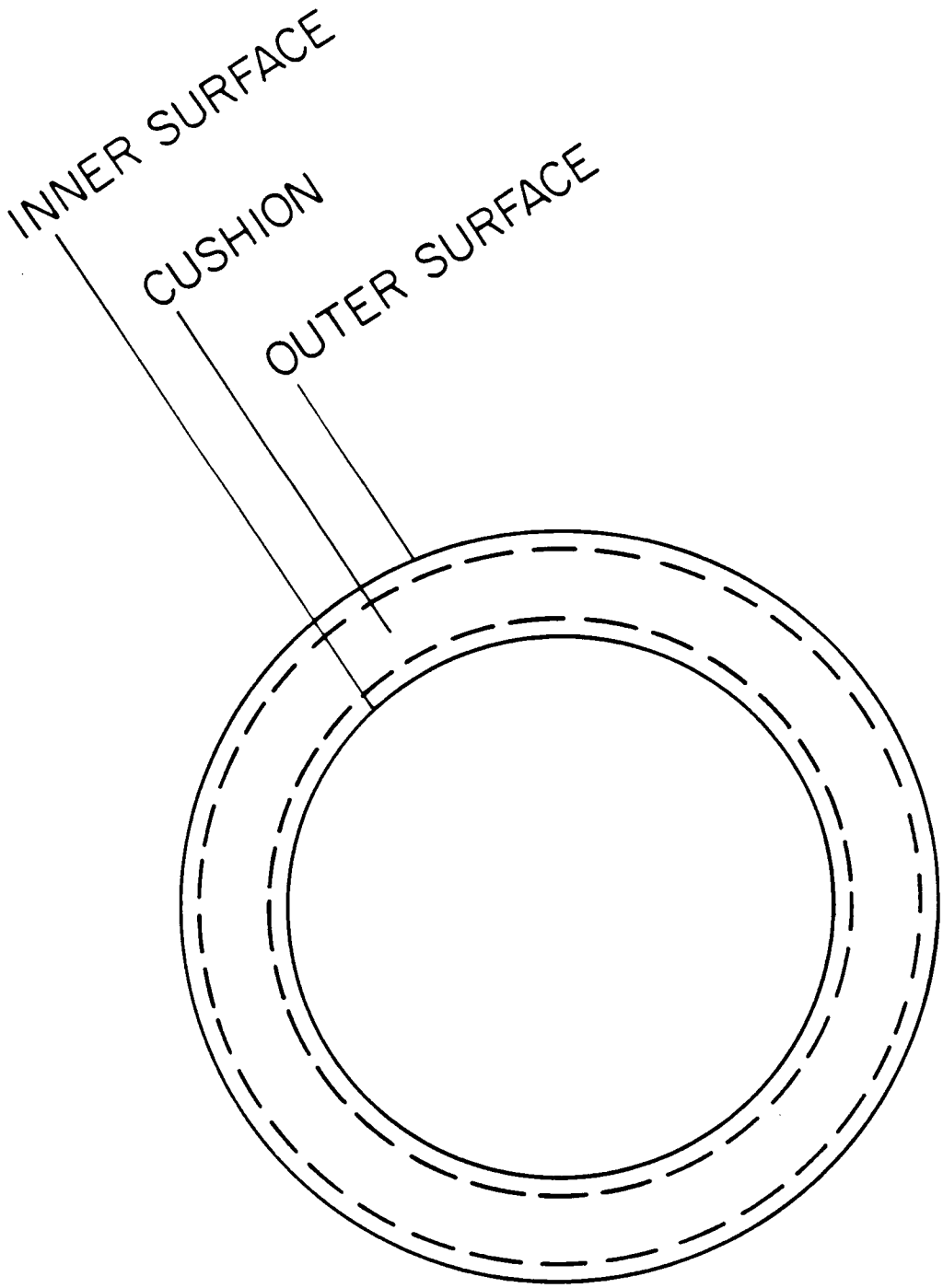

APPENDIX 16

PHYSICS OF THE X-RAY LASER IN A SPACE-BASED BALLISTIC MISSILE DEFENSE

II. Uses of the X-ray Laser in a Missile Defense

Crockett Grabbe

Department of Physics

University of Iowa

Iowa City, IA 52242

ABSTRACT

The basic physics of proposed uses of the nuclear-explosion pumped X-ray laser in a defense against ballistic missiles is analyzed. A calculation is made of the rise time necessary as a function of fuel mass for X-ray laser rockets to reach adequate heights for destroying Soviet missiles exiting the atmosphere in the boost phase. This shows it will not be useful for a boost-phase defense. This result plus the potential countermeasure for midcourse warheads imply that the only viable missile defense uses for this devise are interactive discrimination and the destruction of decoy balloons in the midcourse. Possible Soviet counters to the latter use are mentioned. Finally, the feasibility of its use as an anti-satellite weapon is discussed.

I. Introduction

In the previous paper (hereafter referred to as I) physical principles were used to determine the basic conditions and requirements that must be met to use a nuclear-explosion pumped X-ray laser as a defense against ballistic missiles (Grabbe 1989). The physics of a defense utilizing the X-ray laser for this purpose is analyzed in this paper.

In section II the proposed "pop-up" defense utilizing the X-ray laser to counter missiles in their boost phase is analyzed. In Section III uses of the X-ray laser defense in the midcourse to counter re-entry vehicles is considered. Section IV discusses how an effective defensive weapon for the midcourse phase would make it an even more effective anti-satellite weapon.

II. Minimum Height and Rise Time for the Boost Phase Defense

To deploy X-ray lasers on space platforms in near-Earth orbit, similar to the proposed deployment of a chemical laser defense, would present a difficulty. Having such weapons in low Earth orbit makes them vulnerable to anti-satellite attack by the offensive, and space mines which could render them inoperative. Also there is the danger that detonation of the nuclear explosion in one of the lasers could severely damage nearby unexploded stations because of the intense X-rays, blast, and heat from the explosion. Low-Earth orbit deployment of the X-ray laser is not a viable basing mode for the X-ray laser.

The proposal to use the X-ray lasers in the boost phase is to base the X-ray lasers on a "pop-up" defense: rockets based on submarines in the ocean to be "popped up" into space upon the notice of an attack. This option is not a feasible one for chemical lasers designed for a

boost-phase defense because the very heavy payload weight will require rockets that are much too large to be launched from submarines (Grabbe 1988). The X-ray lasers, however, have a relatively lightweight payload. Critical components in such a defense are the time necessary to launch the laser rockets to an adequate height to counter the missiles, and the mass of the fuel that is required to power the rocket to its firing range.

One can determine the minimum height the X-ray laser rockets must rise in order to be able to hit the missiles over the Earth's curvature and atmosphere by using the basic geometry shown in Figure 1. The submarine must be based in the Indian Ocean for a closest approach to the missiles, and the missiles will be assumed to take off at their present launch angle of 23^{o} with respect to the Earth's surface. This angle is chosen to minimize the fuel needed for the ICBM's. It could be lowered if the Soviets design of a new kind of booster with larger fuel tanks, so the missiles would spend a greater amount of time in the atmosphere.

The X-ray laser beam cannot penetrate the atmosphere below about 100 km, so the line between it and the missile it targets has to be above that. What has been drawn is a minimum height for the X-ray laser rocket to hit the target right at the end of the boost phase and for the X-ray beam to be just barely above (grazing) the atmosphere at its closest approach. In reality it may have to reach a greater height in order to destroy missiles by the end of the boost phase.

The time required to the X-ray laser rocket to rise to the height necessary to hit the missile can be minimized by choosing the appropriate angle of launch of the rocket. A line has been drawn out radially

from the Earth that intersects the line for a minimum grazing of the atmosphere at point A. The rocket can explode and hit the missile when it reaches this line, and it is obvious that the shortest distance for the rocket to travel to this line occurs for an arrival perpendicular to the line (as a variational calculation could show).

Assume the height of the top of the atmosphere is h, the distance the missile has travelled when it is first subjected to a hit by the X-ray laser is l, the height which the X-ray laser must reach to hit the missile is x, and the angle with respect to the center of the Earth at which the missile launch sight is to the submarines which will launch the X-ray laser is φ. Simple geometry shows that the angle of launch for the rocket is also φ.

Extra lines have been drawn from the center of the Earth, one to the point where the ICBM is when the X-ray laser first hits it (of length of R + y where R = 6400 km is the Earth's radius), and one to the point where the X-ray laser beam is just tangent to the upper atmosphere (of length R + h). The angle the two lines form with each other is denoted by ρ, and the angle the first line forms with the line drawn from the Earth's center to the launch site of the missile is denoted by α. Using basic trigonometric rules for the four triangles in the diagram -- three with one vertex at the Earth's center (two of them are obviously right triangles), and one right triangle with the missile launch site as one vertex and the missile in the target range a second vertex -- we have the following relationships:

$$l = y/\sin 23^{\circ} = 2.56\ y \qquad (1)$$

$$\cos \rho = (R + h)/(R + y) \qquad (2)$$

$$l^2 = R^2 + (R + y)^2 - 2R(R + y)\cos \alpha \quad (3)$$

$$\cos [\varphi - (\rho - \alpha)] = (R + h)/(R + r) \quad (4)$$

$$x = r \cos [\varphi - (\rho - \alpha)] \quad (5)$$

Equation (2) can be re-expressed as the solution for :

$$x = R \{1 - \cos [\varphi - (\rho - \alpha)]\} + h \quad (6)$$

We can also determine the distance z that the beam must travel before it hit the missile once it is fired from the x-ray laser rocket. This is given by

$$z = (R + h - x) \tan[\varphi - (\rho - \alpha)] + (R + h) \tan \rho \quad (7)$$

The X-ray laser rocket requires rapid acceleration to achieve the necessary heights. For an initial simplified calculation we will assume that 10.0 g's is possible, for 0.1 km/sec^2 acceleration. To achieve this acceleration would require a chemical rocket booster.

The length which is ICBM has travelled l and the height it has reached y can be expressed in terms of the acceleration of the ICBM and the time after the launch t_{launch} at which the X-ray laser hits the missile. The acceleration in the upwards direction can be determined to be 36 m/sec^2 (see the Appendix for a calculation of the boost phase dynamics of the missile). The missiles first emerge from the atmosphere at 74 seconds, but the Earth's curvature does not allow the laser to hit the missile until shortly afterward. Taking the Soviet boost phase time as 150 seconds one would want to have the

first X-ray lasers up to hit the missile by 130 seconds at the very latest after the launch to have hope of killing the bulk of the missiles (at least a 90% boost phase kill is required to "break even" after MIRVing). It will take at least 30 - 60 seconds for the launch to be detected, communication to the submarine to be made, and preparation for the launch to be made (including possibly time for the submarines to surface). Thus the missile will have at most 75 - 100 seconds rise time to hit the missile.

Thus 100 seconds will be used in the calculations for the time necessary for the X-ray lasers to be accessible to the missiles. The angle at the center of the Earth between the submarines and the missiles varies running from about 35 degrees at a minimum to well over 45 degrees at a maximum. The three angles of 35, 40, and 45 degrees have been chosen to represent this range.

In Table 2 the solution for x is presented for the three values of φ. It is seen that in general the minimum height needed for the X-ray laser to have any hope of destroying the ICBM is in the 1000-2000 km range, and the rise time t_{rise} of which is around is in the 132-169 seconds range. Not only does this exceed the 100 second maximum time needed to allow reasonable kill time to destroy the missiles, but it can even exceed the total boost phase time of the missile. Furthermore the 150 second boost phase time assumed here will be available to the Russians when they reach our present state of missile technology. (The US has 150 second boost phase time missiles.) After that technological developments by them will allow even that to be shortened considerably, probably by the time the US has researched and built a space missile defense.

TABLE 2:

X-ray Laser Rise Times

φ (deg)	35	40	45
t_{launch} (sec)	100	100	100
y (km)	204	204	204
l (km)	522	522	522
ρ (degs)	10.18	10.18	10.18
α (deg)	4.24	4.24	4.24
r (km)	1036	1446	1971
x (km)	907	1199	1532
t_{rise} (sec)	132	150	169
Firing distance (km)	4277	4754	5202

The above equations can also be used in a more realistic calculation to put an estimate on the minimum acceleration and minimum final velocity that will be required in order for the rocket to reach the required altitude in sufficient time to destroy a substantial portion of the missiles in the boost time to destroy a substantial portion of the missiles in the boost phase. This can then be used to determine the ratio of the mass of the fuel required to power the rocket to the mass of the x-ray laser payload that must be delivered to the appropriate height, as was done in Bethe and Garwin (1985). This is done through the standard rocket equation of motion (Langton 1970):

$$m\, dv/dt = v_e\, dm/dt + mg - \beta v \qquad (8)$$

where m is the mass of the rocket, v its velocity and β the frictional coefficient. The first term on the right-hand side is the exhaust velocity v_e multiplying the rate of change of the mass, the second the gravitational attraction on the rocket, and the third the friction of air. The first term is much larger than the second two, so the latter terms will be neglected. Then equation (8) integrates to the form

$$m_f/m_i = \exp(v_f/v_e) \qquad (9)$$

where m_i is the initial mass (rocket + fuel), and m_f and v_f are the final rocket mass and velocity. Knowing the exhaust velocity for the fuel and the minimum final velocity of the missile required for it to reach the required height in time for a boost phase defense, one can determine the ratio of the initial mass (fuel plus payload) for the

missile to the final mass (payload) of the X-ray rocket.

For a boost phase defense the rocket must achieve a high rate of acceleration to reach the heights required in the short time available. The only engines that could feasibly achieve this acceleration is the chemical engine. Such engines have a typical exhaust velocity of around 3 km/sec, and can only produce a maximum exhaust velocity of around 5 km/sec (Langton 1970). We will assume the latter can be achieved for an X-ray laser rocket.

Table 3 contains results for the minimum acceleration necessary for the rocket to reach the required height. The cases in which 75 and 100 seconds is available for the rise time correspond to a 150 second boost phase time with 30 - 60 seconds time for detecting, alerting, and preparing for the attack. If the Soviet reduce their boost phase time to 100 seconds, at most 50 seconds would be available for the rise, so that case has also been included. Also shown is the mass ratio of the fuel to the payload required for the rocket.

If the payload of the rocket has a mass of 1000 kilograms (just over a ton), the fuel required for the missile is 32,000 kilograms for the most optimum case (countering the most southern Soviet missiles in the case of 100 second rise time available for the rocket). This corresponds to a missile weight not more than a factor of 2 larger than current submarine missiles. However, the other cases are all orders of magnitude larger than what a submarine could carry and launch. In general, the rockets with the required conditions necessary for a boost-phase intercept cannot be built for submarine basing.

These calculations show that the X-ray laser will be basically useless as a boost phase defense.

Table 3:

Acceleration Rate and Mass Ratios Required for Interception

φ	t(sec)	a (km/sec)	m_i/m_f
35	50	697	1,075
35	75	309	103
35	100	174	32
40	50	886	7,040
40	75	394	369
40	100	222	85
45	50	1,142	8.30×10^8
45	75	508	2,039
45	100	286	305

III. Using the X-ray Laser in the Midcourse

The rise time of the X-ray rocket nullifies the hope of using it for a boost-phase defense. There is an interest in using it in the midcourse, however since the rise-time factor is not so critical there. In this phase the warheads of missiles that have survived the boost phase and undergone MIRVing (deployment of their multiply-independent re-entry vehicles) are on a ballistic course toward the United States. They will be harder to destroy than the missiles were in boost phase for the following reasons:

1. The RVs are much smaller than the missiles and harder to hit.
2. The missiles could be taken out by damaging their very vulnerable fuel tanks to prevent them from attaining adequate final velocity to reach their destination, or by destroying them by exploding the tank. The warheads, on the other hand, are much harder to destroy since they are hardened to withstand the high heat in the re-entry conditions. It will require at least an order of magnitude greater energy intensity to destroy the RVs than the booster.
3. For every missile not taken out of action in the boost phase, 10 MIRVed warheads are produced. These 10 objects are each much more difficult to destroy than the missile from which they originated.
4. When the MIRVed warheads are deployed about 20 times as many balloons could be deployed as decoys (since the weapons are in free space the balloons travel right along with the warheads). The warheads can be hidden in the balloons and the defense must destroy all the balloons to expose the warheads before they can target them, or else have a means of detecting which balloons have the warheads.

The countermeasure of shielding the RV, such as by putting protec-

tive outer coatings on it as discussed in I, will likely be adequate to shield it from the laser in the midcourse. There are 2 things thing the laser might be useful for in the midcourse. One is to destroy the decoy balloons and expose the warheads, since the balloons cannot be as easily shielded. The other is to use them in an interactive discrimination role to identify which balloons contain actual warheads.

The use of the laser for interactive discrimination in the midcourse is promising if several beams are used from a single X-ray laser. However, a calculation of the requirements for this case shows that several hundred independently targetable laser rods will be required per X-ray laser, and as many independent X-ray laser platforms as there are missiles which survive the boost and post-boost phases (American Physical Society 1987).

The Soviets would have the advantage of the surprise of the launch, the exact timing of the launch, and when and where the RVs will pass by. They could have submarines stationed along the precisely planned path at that time. These submarines could send up X-ray lasers just when the warheads are in range and the US X-ray lasers launched. The X-ray lasers could be directed to destroy our X-ray laser rockets as they leave the atmosphere.

The objective would be to destroy virtually all the balloons so all the warheads could be exposed. If it could not be done many warheads would get through the midcourse, and would have to be taken out in the 1 to 2 minutes available to do that in the terminal phase. However, the Soviet goal will only be to partially destroy the X-ray lasers. Doing so would ensure a large portion of the balloons would not be destroyed, which is all that would be needed to ensure some of the warheads get through.

In summary, the X-ray lasers would probably not be adequate to do a complete job of that if the Soviets take an active course in countering their deployment. Thus other means of destroying the balloons or detecting which balloons have the warheads would also have to be utilized.

IV. The X-ray Laser as an Antisatellite Weapon

In addition to its feasible use to counter midcourse balloons the X-ray laser could be quite effective as an anti-satellite weapon in general. Satellites are an essential part of the nuclear force. The functions they perform in this capacity are early warning against a Soviet nuclear attack, spying on Soviet military developments, verifying that the Soviets are complying with nuclear treaties, and worldwide communication of the naval forces. These uses are stabilizing in the nuclear arena, helping to make the onset of a nuclear war less likely.

Part of the advantage the X-ray laser has when used in this mode is that of surprise. Offense always has the advantage of surprise. When the X-ray laser is used in a defensive mode it must receive the warning from the early-warning satellites and locate and track the missiles. We have shown it is too slow to attack the missile in the boost phase, so it must track all the RVs produced in MIRVing. All this information must be obtained and the laser rockets readied and fired in a few short minutes. Finally, the lasers rockets themselves will be subject to attack.

Used in the anti-satellite mode, the path of the satellite will be known well ahead of time. It can be used to spring an attack on the satellite, and it is much harder to protect a satellite against the

surprise attack. The X-ray laser has a high lethality, and the satellite has several sensitive systems for which it is easy to achieve the energy intensity to destroy. One of these it the sensitive infrared or optical system used for its function of early-warning, spying, or treaty-verification. The other is its communication system for relaying information it obtains to ground-based stations. This requires appropriate antennas and sensitive electronics. Rendering these sensitive systems inoperative makes the satellite useless in its function.

These facts indicate that the X-ray laser is much more effective as an anti-satellite system than as a defense against missiles.

ACKNOWLEDGMENTS

This work was supported in part by grant NAGW-827 with the National Aernautics and Space Administration of the United States.

Appendix:

Dynamics of a Missile in the Boost Phase

Let h_b be the height of the reached at the end of the boost phase, and t_b be the boost phase time. Thus the height the missile attains in the boost phase is given by:

$$at_b^2/2 = h_b \tag{A1}$$

where a is the component of rocket acceleration in the upwards direction (which is offset by the gravitational acceleration g). In addition the final velocity component in the upward (radial) direction of the rocket when the boost phase ends v_f is given by

$$at_b = v_{fr} \tag{A2}$$

v_{fr} is known and can be determined by the fact that the total (kinetic plus potential) energy of the rocket must remain the same when it reaches it maximum height h_{max} in its whole course of flight to the United States, at which point the v_{fr} is zero and it has only a gravitational potential. Because h_{max} is large compared to the radius R of the Earth, the radial forms of potential energy must be used. Since $h_b \ll R$ we have:

$$mv_{fr}^2/2 - mMG/R = -mMG/(R + h_{max})$$
$$v_{fr} = [2(MG/R^2)h_{max}/(1 + h_{max}/R)]^{1/2} \tag{A3}$$

$MG/R^2 = g = 9.8$ m/sec^2 is just the gravitational acceleration rate at the Earth's surface. For ICBM's $h_{max} = 2000$ km, yielding

$$v_{fr} = 5{,}465 \text{ m/sec} \tag{A4}$$

From equations (A1) and (A2) we have the final velocity and acceleration, assuming the boost phase ends at $t_b = 150$ sec. (the Soviets will be able to achieve boost phases of this time when their missile technology catches up with the US present technology):

$$h_b = t_b v_{fr}/2 = 410 \text{ km} \tag{A5}$$
$$a = v_{fr}/t_b = 36.4 \text{ m/sec}^2$$

The X-ray laser cannot counter the missile until it leaves the atmosphere. The time at which the missile exits the atmosphere after it is launched can be similarly determined. One has

$$at_a^2/2 = h_a \tag{A6}$$

where h_a is the height of the atmosphere, and t_a is the time from the launch to the atmosphere exit. Using $h_a = 100$ km and the value for a from above one has

$$t_a = 74.1 \text{ sec.} \tag{A7}$$

as the time necessary before the missile leaves the atmosphere.

REFERENCES

American Physical Society Study Group Report, 1987 (3) Science and Technology of Directed Energy Weapons Rev. Mod. Phys. 59 Part II S1-S202

Bethe H and Garwin R 1985 (1) Weapons in Space Vol 1 Daedalus 346-352

Grabbe C L 1989 submitted to Eur. J. Phys.

Grabbe C L 1988 Amer. J. Phys. 56, 32

Langton N H 1970 Rocket Propulsion (New York: American Elsevier) chap. 2.

FIGURE CAPTION

Figure 1. Geometry of the shooting of an X-ray laser to the minimum height necessary for the laser beam to be able to pass over the atmosphere and hit the missile in its boost phase.

A-G86-566-I

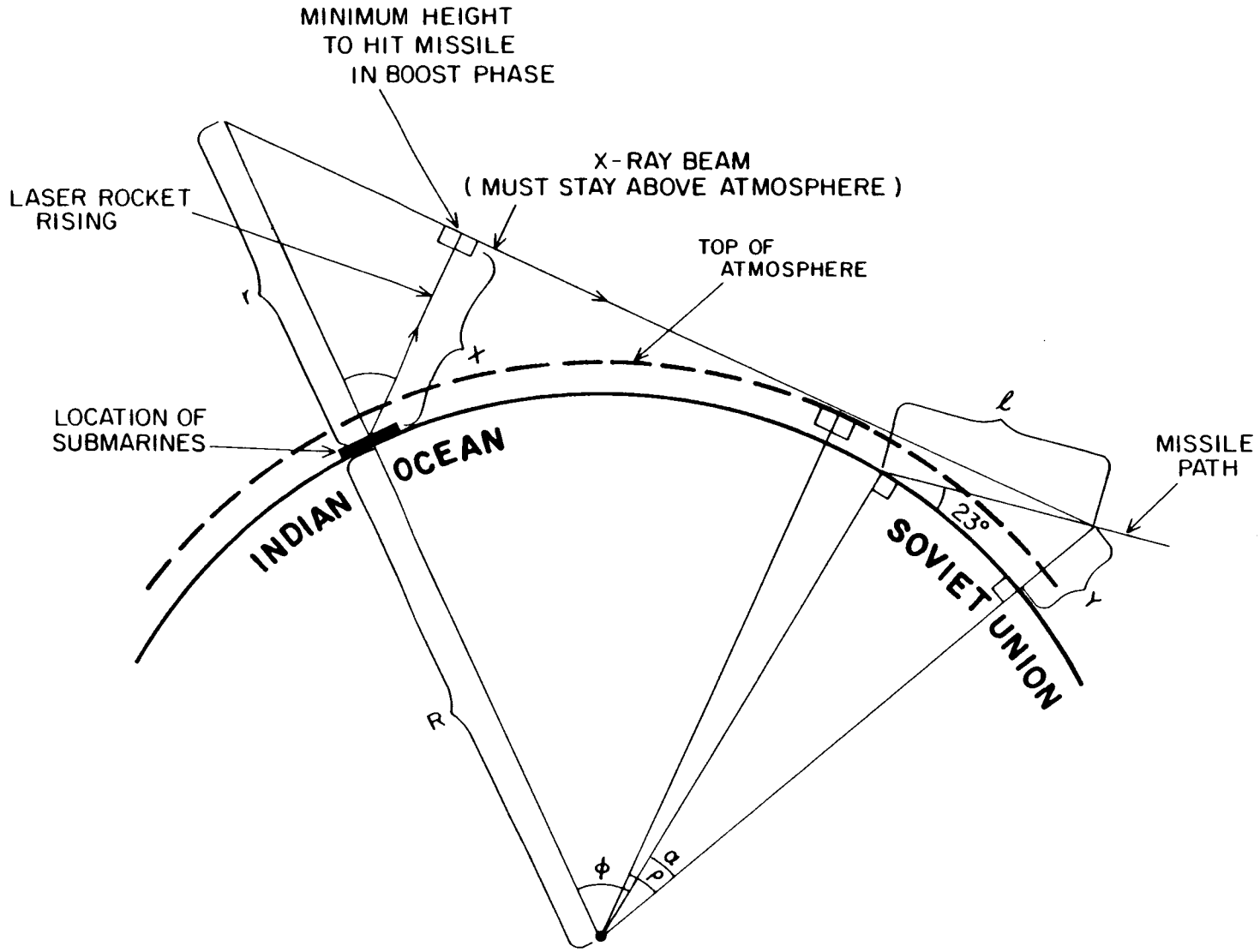
MINIMUM HEIGHT
TO HIT MISSILE
IN BOOST PHASE
X-RAY BEAM
(MUST STAY ABOVE ATMOSPHERE)
LASER ROCKET
RISING
TOP OF
ATMOSPHERE
r
x
LOCATION OF
SUBMARINES
INDIAN
OCEAN
ℓ
MISSILE
PATH
23°
SOVIET UNION
y
R
ϕ
α